Microwave Engineering
Ulm University

universität
ulm

Influence of Ramp Timing Dither on Modulation-Based Radar Target Simulators

Pirmin Schoeder, Vinzenz Janoudi, Timo Grebner, Arne Martin, and Christian Waldschmidt

European Microwave Week 2022 Conference Proceedings. ©EuMA 2022.
Materials contained in the European Microwave Week 2022.
DOI: 10.23919/EuRAD54643.2022.9924807
ISBN: 978-2-8748-7071-2

Influence of Ramp Timing Dither on Modulation-Based Radar Target Simulators

Pirmin Schoeder, Vinzenz Janoudi, Timo Grebner, Arne Martin, Christian Waldschmidt
Institute of Microwave Engineering, Ulm University, Germany
{name.surname}@uni-ulm.de

***Abstract* — For the development of fully-autonomously driving vehicles, advanced test capabilities for sensor systems are required. With modulation-based radar target simulators, complex traffic scenarios can be simulated for automotive radars at low costs. Yet the simulation principle relies on the timings of the chirp-sequence frequency modulated continous waveform. Since small timing variations can be purposely introduced on the radar's waveform e.g. for interference mitigation techniques, the assumption of ideal timings could be violated. Therefore, this paper investigates the influences of ramp timing deviations on the target simulation. A signal model for radar timing variations for modulation-based simulators is presented. Furthermore, the influence of ramp timings on the resulting signal-to-noise ratio of simulated target responses is derived and verified by measurements.**

***Keywords* — automotive radar, chirp-sequence modulation, FMCW radar, radar target simulator, system modelling.**

I. Introduction

With the ever increasingly complex tasks that advanced driver assistance systems (ADAS) have to accomplish, the need to test and verify their functionality in special traffic scenarios arises. Since many systems rely on radar imaging due to its high reliability [1], [2], a test bench, capable of simulating complex traffic scenarios for radar sensors, helps to shorten development cycles and to enhance the safety of ADAS. Modulation-based radar target simulators (RTSs) offer a cost-effective way to simulate many targets for an automotive chirp-sequence frequency modulated continous wave (CS-FMCW) radar sensor [3]–[6]. The modulation-based architecture employs a signal source which modulates the radar transmit signal in order to simulate targets with a velocity and distance. Furthermore, arbitrary directions-of-arrival of targets can be simulated, by combining multiple modulation-based RTSs [7]. The modulation principle relies on the frequency ramp timings of the CS-FMCW waveform. So far, current research considered only perfectly timed frequency ramps [3]–[7]. Since the application of dithered ramp timings (ramp timings with a random component) is an effective solution for interference mitigation [8], [9], and recommended by radar chip manufacturers [10], the influence of ramp timing deviations on the target simulation is of high interest. In order to assess the influence of deviations from an ideally timed CS-FMCW waveform, this paper mathematically derives the effects of randomized ramp timings. The paper is structured as follows: First, the general working principle of modulation-based target simulators is presented. Afterwards a mathematical model that considers ramp timing deviations and their influence on the resulting range-Doppler information is derived. Lastly, the models for the resulting signal-to-noise ratio (SNR) are verified by radar measurements.

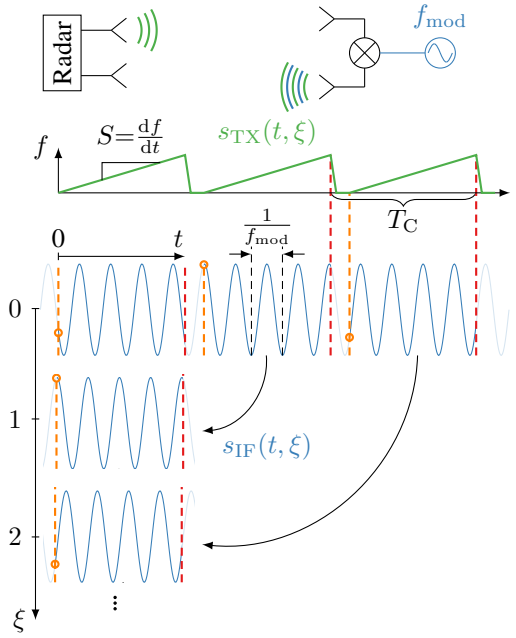

Fig. 1. The working principle of a modulation-based RTS with ideal ramp timings T_{C}

II. Working Principle of Modulation-Based Target Simulators

CS-FMCW radar sensors measure the traveled distance of a reflected wave by measuring the frequency difference between the transmit- and receive signal. Therefore, an RTS that applies a CW frequency shift can simulate a radar target with a range component. Since a frequency shift can either in- or decrease the frequency, positive and negative range shifts are feasible. In the following we assume a chirp sequence radar with an up-chirp, so the frequency of the CW signal increases. Due to the increasing frequency of the transmit signal, a delay in the channel causes a lower frequency of the received chirp compared to the transmitted chirp at the same time instance. Hence, an RTS has to shift the chirp to a lower frequency in order to simulate a positive range. Furthermore, the radial velocity of a target with respect to the radar is determined by

the distance the target travels during multiple chirps, which causes a phase shift between the ramps. It was shown in [3] that applying a frequency shift to the radar transmit signal of

$$f_{\mathrm{mod}} = \frac{1}{T_{\mathrm{C}}} \left\lfloor \frac{2RST_{\mathrm{C}}}{c_0} \right\rceil + f_{\mathrm{D}}\,, \tag{1}$$

allows the simulation of both properties—range R and a Doppler shift of f_{D}—where $\lfloor \cdot \rceil$ denotes rounding to the nearest integer, S is the slope of the radar's frequency ramp, and T_{C} is the chirp repetition period. The resulting complex-valued intermediate frequency (IF) signal s_{IF} after the down-conversion at the radar receiver for the ξ-th ramp, neglecting the physical distance between radar and simulator, is calculated as

$$\begin{aligned} s_{\mathrm{IF}}(t,\xi) &= \exp\left(\mathrm{j}2\pi \left(\frac{1}{T_{\mathrm{C}}} \left\lfloor \frac{2RST_{\mathrm{C}}}{c_0} \right\rceil + f_{\mathrm{D}}\right) \cdot (t + \xi T_{\mathrm{C}})\right) \\ &\approx \exp\left(\mathrm{j}2\pi \left(\frac{2RS}{c_0} t + f_{\mathrm{D}} \xi T_{\mathrm{C}} + \xi \left\lfloor \frac{2RST_{\mathrm{C}}}{c_0} \right\rceil\right)\right) \\ &= \exp\left(\mathrm{j}2\pi \frac{2RS}{c_0} t + j2\pi f_{\mathrm{D}} \xi T_{\mathrm{C}}\right)\,. \end{aligned} \tag{2}$$

Where t indicates the intra-chirp timing from 0 to the duration of the up-chirp. The slope of the frequency ramp S and chirp repetition period T_{C} have to be known or can be estimated with sufficient accuracy [4]. Due to the modulation principle, a single modulation frequency leads to a target with a simulated range R and velocity v. Due to the undersampling of the modulation frequency by the ramp timings ξT_{C}, a defined phase shift between ramps can be set. Both, the radar and the modulation source are running independently and no trigger is required. In Fig. 1 the IF signal is depicted that results from a modulation-based simulation with ideal ramp timings T_{C}.
By superimposing multiple (K) modulation signals with amplitude A_k and frequency $f_{\mathrm{mod},k}$, K targets are simulated simultaneously. The receive signal of the radar, after being modulated is described by

$$\begin{aligned} s_{\mathrm{RX}}(t,\xi) =& s_{\mathrm{TX}}(t,\xi) \cdot \sum_{k=1}^{K} A_k \exp(-\mathrm{j}2\pi f_{\mathrm{mod},k}(t + \xi T_{\mathrm{C}})) \\ &+ n(t,\xi)\,, \end{aligned} \tag{3}$$

where $n(t,\xi)$ is complex-valued white Gaussian noise. Each of the K sinusoids causes an IF signal as in (2). Hence, in the following the analysis of the IF signal is conducted for a single simulated target. In the case of a simulated multi-target scenario, the target-individual IF signals with timing deviations are superimposed.

III. Impact of Ramp Timing Dither

Ramp timing deviations lead to non-periodic transmission intervals of individual chirps of the CS-FMCW waveform. Fig. 2 shows the conceptual consequence of dithered ramp timings. A varying ramp starting time, leads to a changing relative phase of the modulation signal that is observed during this ramp. So in order to model dithered ramp timings that deviate from the ideal ramp timing T_{C} in (2), the IF signal of the radar is expanded by the timing deviations $\Delta T(\xi)$ and changes therefore to

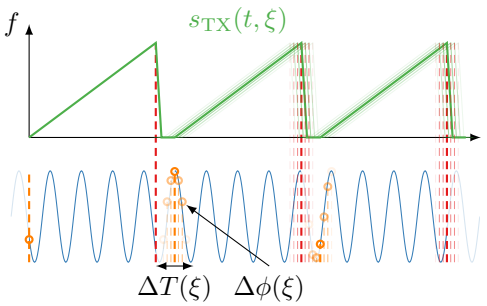

Fig. 2. Schematic illustration of ramp timing deviations $\Delta T(\xi)$ leading to phase deviations $\Delta\phi(\xi)$ with the modulation-based simulation approach.

$$\begin{aligned} \widetilde{s}_{\mathrm{IF}}(t,\xi) &= \exp\Big(\mathrm{j}2\pi f_{\mathrm{mod}}\big(t + \xi T_{\mathrm{C}} + \Delta T(\xi)\big)\Big) \\ &= \exp\Big(\mathrm{j}2\pi f_{\mathrm{mod}} t \\ &\quad + \mathrm{j}2\pi \frac{\xi T_{\mathrm{C}} + \Delta T(\xi)}{T_{\mathrm{C}}} \left\lfloor \frac{2RST_{\mathrm{C}}}{c_0} \right\rceil \\ &\quad + f_{\mathrm{D}}\big(\xi T_{\mathrm{C}} + \Delta T(\xi)\big)\Big) \\ &= s_{\mathrm{IF}}(t,\xi) \exp\big(\mathrm{j}\Delta\phi(\xi)\big)\,. \end{aligned} \tag{4}$$

The phase error $\Delta\phi(\xi)$ that results from the ramp timing deviation $\Delta T(\xi)$ is

$$\begin{aligned} \Delta\phi(\xi) &= 2\pi \frac{\Delta T(\xi)}{T_{\mathrm{C}}} \left(\left\lfloor \frac{2RST_{\mathrm{C}}}{c_0} \right\rceil + \frac{f_{\mathrm{D}}}{T_{\mathrm{C}}}\right) \\ &\approx 2\pi \frac{\Delta T(\xi)}{T_{\mathrm{C}}} \left\lfloor \frac{2RST_{\mathrm{C}}}{c_0} \right\rceil\,. \end{aligned} \tag{5}$$

The relation between the ramp timing deviations ΔT and resulting phase shift of s_{IF} is nonlinear due to the $\exp(\cdot)$ function in (4).
With the aim of simplifying the model, the exponential function in (4) is approximated by its first order Taylor series

$$\exp(\mathrm{j}\Delta\phi(\xi)) \approx 1 + \mathrm{j}\Delta\phi(\xi)\,. \tag{6}$$

The fully linearized description of the IF signal is therefore

$$\begin{aligned} \widetilde{s}_{\mathrm{IF}}(t,\xi) &= s_{\mathrm{IF}}(t,\xi) + \mathrm{j}s_{\mathrm{IF}}(t,\xi) \frac{2\pi\Delta T(\xi)}{T_{\mathrm{C}}} \left\lfloor \frac{2RST_{\mathrm{C}}}{c_0} \right\rceil \\ &= s_{\mathrm{IF}}(t,\xi) + N(\xi)\,. \end{aligned} \tag{7}$$

Equation (7) reveals that the additive noise $N(\xi)$ scales directly with the amplitude of the IF signal. The resulting block diagram of the linearized model is depicted in Fig. 3.
If the ramp timing deviations ΔT are generated by a random

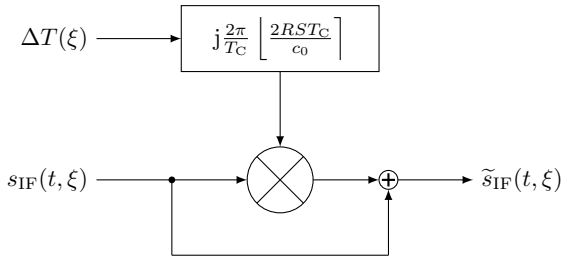

Fig. 3. Block diagram of resulting model for ramp timing deviations ΔT of a target with simulated range R.

process and have an expected value of $\mathrm{E}\{\Delta\mathrm{T}\}=0$, the power of N is calculated as

$$\mathrm{E}\{NN^*\}=P(s_\mathrm{IF})\frac{4\pi^2\mathrm{Var}(\Delta T)}{{T_\mathrm{C}}^2}\left\lfloor\frac{2RST_\mathrm{C}}{c_0}\right\rceil^2. \quad (8)$$

The symbol * denotes the complex conjugate operation. Again, it can be seen that the power of the additive noise scales linearly with the power of the IF signal $P(s_\mathrm{IF})$. The ramp timing deviations are assumed to be generated by the radar's timing engine via a white process. Ramp timing dither from a white process is favorable for the radar design, as for example in interference scenarios, no correlations can occur between interferer and victim [9]. Since the generating process is white, the noise power is distributed equally over all velocity bins and the SNR within the Rv-bin of the target due to the ramp timing deviations is

$$\mathrm{SNR}=\frac{{T_\mathrm{C}}^2}{4\pi^2\mathrm{Var}(\Delta T)}\left\lfloor\frac{2RST_\mathrm{C}}{c_0}\right\rceil^{-2}\Xi. \quad (9)$$

Where Ξ is the number of evaluated frequency ramps. From (9) can be seen that doubling the simulated range R decreases the SNR by 6 dB for a given variance of ramp timing deviations $\mathrm{Var}(\Delta T)$. Vice versa, (9) can also be used to calculate the maximum timing variance, for a guaranteed $\mathrm{SNR}_\mathrm{min}$ with given radar parameters

$$\mathrm{Var}(\Delta T)\leq\frac{{T_\mathrm{C}}^2}{4\pi^2\mathrm{SNR}_\mathrm{min}}\left\lfloor\frac{2RST_\mathrm{C}}{c_0}\right\rceil^{-2}\Xi. \quad (10)$$

With the aim to guarantee a proper simulation, ramp timing randomizations should therefore be turned off completely on the radar side, if a modulation-based RTS is used. The simulated range on the other hand is unaffected, since it only depends on the intra-chirp timing t and is therefore independent of chirp timing variations ΔT.

IV. Measurements

In order to verify the presented model for the influence of radar ramp timing deviations, measurements were performed in an anechoic chamber. The measurement setup with the RTS and radar is depicted in Fig. 4. The RTS was utilized to simulate K=6 targets. The simulated distance is doubled for each target R_k=1 m, 2 m, 4 m,..., 32 m, thus approximately doubling the modulation frequency $f_{\mathrm{mod},k}$ from target to target. A maximum of Ξ=32 chirps with individual ramp

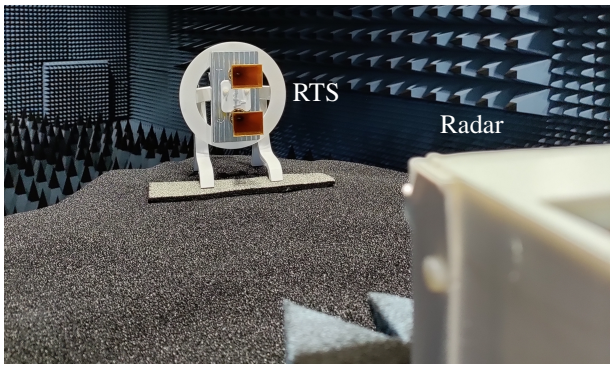

Fig. 4. Photograph of the setup for radar measurements with the radar target simulator.

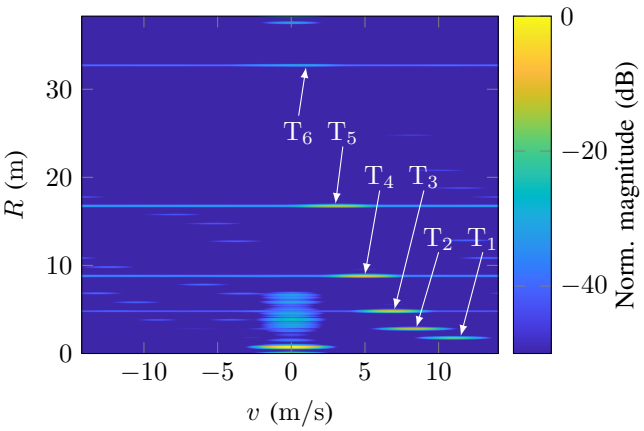

Fig. 5. Resulting Rv-plot averaged over 200 frames with dithered ramp timings, normalized to the target of the RTS itself.

timings can be transmitted by the radar within a single frame. All important radar parameters are listed in Table 1. The applied ramp timing dither $\Delta T(\xi)$, generated by a white process is uniformly distributed in the interval between −25 ns and +25 ns at a ramp repetition period of T_C=67 µs. For the purpose of estimating the SNR of the individual targets, 200 radar frames with different ramp timing dither realizations were observed and the average magnitude of the resulting Rv data is calculated, which is depicted in Fig. 5. The increasingly elevated noise floor with higher modulation frequencies is clearly visible. The target T_6 can barely be distinguished from the elevated noise floor, as its SNR decreased to 10 dB.
To compare the signal model of this paper to the measured results, the expected relative noise floor of the R=const.-cuts at the simulated targets' range is depicted in Fig. 6. The expected noise floor is the sum of the estimated additive white

Table 1. Overview of the radar parameters

Ramp duration T_c	67.0 µs
Variance of timing deviations $\mathrm{Var}(\Delta T)$	$2.08\times10^{-16}\,\mathrm{s}^2$
Number of ramps Ξ	32
Start frequency	77.2 GHz
Bandwidth B	2 GHz
Frequency slope S	39.1 MHz/µs

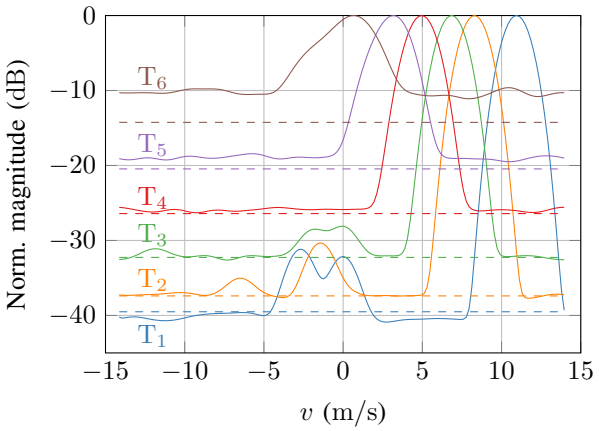

Fig. 6. Estimated noise level for each modulation frequency in dashed lines and the v-plane cuts at the simulated target distance, normalized to each maximum.

Gaussian noise $n(t,\xi)$ of the radar itself and the additional white noise $N(\xi)$ due to the ramp timing dither according to (9). The radar-inherent noise floor is estimated by the median magnitude for each R=const.-cut without stationary targets of the Rv data. For the target T_1, the radar-inherent noise $n(t,\xi)$ is the predominant one. For the targets T_2 to T_6, the noise due to ramp deviations $N(\xi)$ dominates. Overall, the estimated noise floor matches for targets with lower simulated ranges to the measured one. For the targets with the largest simulated distances T_5 and T_6, the linearization in (6) becomes inaccurate and the measured noise floor is significantly higher than is expected from the linearized model. This is also evident in the broader target peaks. The 3 dB-width compared to T_1 is increased by 30 % and 100 % for T_5 and T_6 respectively. The additional peaks in Fig. 6 at v=0 m/s are reflections caused by the anechoic chamber, peaks at velocity $v\neq$0 m/s stem from harmonics of the modulation signal.

V. Conclusion

In this paper, the effects CS-FMCW ramp timing deviations on modulation-based radar target simulators are analyzed. A signal model is derived that describes the additional noise, which is caused by purposely introduced randomizations of the chirp transmit timings. By simulating a scenario with multiple targets, the influence of the correct prediction of the resulting noise from ramp timing variations could be proven. In order to guarantee a sufficient SNR, dithered ramp timings should be avoided or kept at a certain maximum value, which can be calculated with the provided model.

Acknowledgment

This work was supported by the German Federal Ministry of Education and Research through the project SecForCARs under grant 16KIS0797.

References

[1] J. Dickmann, J. Klappstein, M. Hahn, N. Appenrodt, H. Bloecher, K. Werber, and A. Sailer, "Automotive radar the key technology for autonomous driving: From detection and ranging to environmental understanding," in *IEEE Radar Conf. (RadarConf)*, 2016, pp. 1–6.

[2] J. Hasch, E. Topak, R. Schnabel, T. Zwick, R. Weigel, and C. Waldschmidt, "Millimeter-wave technology for automotive radar sensors in the 77 GHz frequency band," *IEEE Trans. on Microw. Theory and Techn.*, vol. 60, no. 3, pp. 845–860, 2012.

[3] J. Iberle, P. Rippl, and T. Walter, "A near-range radar target simulator for automotive radar generating targets of vulnerable road users," *IEEE Microw. and Wireless Compon. Lett.*, vol. 30, no. 12, pp. 1213–1216, 2020.

[4] P. Schoeder, B. Schweizer, A. Grathwohl, and C. Waldschmidt, "Multitarget simulator for automotive radar sensors with unknown chirp-sequence modulation," *IEEE Microw. Wireless Compon. Lett.*, vol. 31, no. 9, pp. 1086–1089, 2021.

[5] W. Scheiblhofer, R. Feger, A. Haderer, and A. Stelzer, "A low-cost multi-target simulator for FMCW radar system calibration and testing," in *Eur. Radar Conf. (EURAD)*, 2017, pp. 343–346.

[6] F. Rafieinia and K. Haghighi, "ASGARD1: A novel frequency-based automotive radar target simulator," in *IEEE MTT-S Int. Conf. on Microw. for Intell. Mobility (ICMIM)*, 2020, pp. 1–4.

[7] P. Schoeder, V. Janoudi, B. Meinecke, D. Werbunat, and C. Waldschmidt, "Flexible direction-of-arrival simulation for automotive radar target simulators," *IEEE J. Microwaves*, vol. 1, no. 4, pp. 930–940, Oct. 2021.

[8] M. Kunert, "MOSARIM - Project Final Report - Publishable summary," Tech. Rep., Dec. 2012.

[9] S. Alland, W. Stark, M. Ali, and M. Hegde, "Interference in automotive radar systems: Characteristics, mitigation techniques, and current and future research," *IEEE Signal Process. Mag.*, vol. 36, no. 5, pp. 45–59, 2019.

[10] *AWR2243 Device Errata Silicon Revisions 1.0 and 1.1*, Texas Instruments Inc., Jan. 2022, rev. B.